Title: Astodrimer sodium, dendrimer antiviral, inhibits replication of SARS-CoV-2 *in vitro.*

Authors: Jeremy R.A. Paull[a,*]; Alex Castellarnau[a]; Carolyn A. Luscombe[a]; Jacinth K. Fairley[a]; Graham P. Heery[a]

Author affiliations:

[a] Starpharma Pty Ltd, 4-6 Southampton Crescent, Abbotsford, Victoria 3067, Australia

* Corresponding author: jeremy.paull@starpharma.com (JP)

Declaration of interest:

The authors declare the following financial interests that may be considered as potential competing interests: J.R.A.P., J.K.F. and G.P.H. are paid employees of Starpharma Pty Ltd. A.C. and C.A.L. are paid consultants to Starpharma Pty Ltd. C.A.L. is a paid employee of Biotron Ltd.

Word count:

Abstract: 273

Text: 2723

Inserts: 1 table, 2 figures

Abstract

An effective response to the ongoing coronavirus disease (COVID-19) pandemic caused by severe acute respiratory syndrome coronavirus 2 (SARS-CoV-2) will require a range of complementary preventive modalities. The current studies were conducted to evaluate the *in vitro* SARS-CoV-2 antiviral activity of astodrimer sodium, a dendrimer with broad spectrum antimicrobial activity, including against enveloped viruses in *in vitro* and *in vivo* models, that is marketed for antiviral and antibacterial applications. We report that astodrimer sodium inhibits replication of SARS-CoV-2 in Vero E6 cells when added to cells 1-hour prior to or 1-hour post infection, with 50% effective concentrations reducing virus-induced cytopathic effect (EC_{50}) ranging from 0.090 to 0.742 µM (0.002 to 0.012 mg/mL). The selectivity index (SI) in these assays was as high as 2197. Astodrimer sodium was also effective in a virucidal evaluation when mixed with virus for 1 hour prior to infection of cells (EC_{50} 1.83 µM [0.030 mg/mL]). Results from a time of addition study, which showed infectious virus was below the lower limit of detection at all time points tested, were consistent with the compound inhibiting early virus entry steps. The data were similar for all investigations and were consistent with the potent antiviral activity of astodrimer sodium being due to inhibition of virus-host cell interactions, as previously demonstrated for other viruses. Further studies will confirm if astodrimer sodium binds to SARS-CoV-2 spike protein and physically blocks initial association of the virus with heparan sulfate proteoglycans on the host cell. Given the *in vitro* effectiveness and significantly high SI, astodrimer sodium warrants further investigation for potential as a nasally administered or inhaled antiviral agent for SARS-CoV-2 prevention and treatment applications.

Keywords: Astodrimer; COVID-19; dendrimer; antiviral; SARS-CoV-2; SPL7013

1. Introduction

The ongoing pandemic coronavirus disease 2019 (COVID-19), caused by severe acute respiratory syndrome coronavirus-2 (SARS-CoV-2) infection, has resulted in unprecedented efforts to rapidly develop strategies to contain infection rates for the protection of vulnerable populations. An effective public health response to the current pandemic will require any vaccine to be supplemented by other alternative preventive modalities.

SARS-CoV-2 receptors and coreceptors have been shown to be highly expressed in nasal epithelial cells (Sungnak et al., 2020). This finding is consistent with the virus infectivity or replication pattern along the respiratory tract, which peaks proximally (nasal cavity) and is relatively minimal in the distal alveolar regions (Hou et al., 2020). These findings suggest that nasal carriage of the virus could be a key feature of transmission, and that nasally administered therapeutic modalities could be potentially effective in helping to prevent spread of infection.

Astodrimer sodium (SPL7013) is a generation -four lysine dendrimer with a polyanionic surface charge (McCarthy et al., 2005) that is active against several enveloped and non-enveloped viruses including human immunodeficiency virus-1 (HIV-1) (Lackman-Smith et al., 2008, Tyssen et al., 2010), herpes simplex virus (HSV)-1 and -2 (Gong et al., 2005), H1N1 influenza virus, human papillomavirus (HPV), adenovirus and Zika virus (unpublished data). Astodrimer sodium also has antibacterial properties. Both size and surface charge contribute to the function of the compound (Tyssen et al., 2010), and when administered topically, astodrimer sodium is not absorbed systemically (Chen et al., 2009; O'Loughlin et al., 2010; McGowan et al., 2011).

Vaginally administered astodrimer sodium protected macaques from infection with chimeric simian-HIV-1 $(SHIV)_{89.6P}$ (Jiang et al., 2005), and mice and guinea pigs from HSV-2 infection

(Bernstein et al., 2003) in vaginal infection challenge models. Astodrimer 1% Gel (10mg/mL astodrimer sodium) administered vaginally has been shown to be safe and effective in phase 2 and large phase 3 trials for treatment and prevention of bacterial vaginosis (BV) (Schwebke et al., 2019; Chavoustie et al., 2020; Waldbaum et al., 2020) and is marketed in Europe, Australia, New Zealand and several countries in Asia.

The current studies were conducted to assess the antiviral activity of astodrimer sodium against SARS-CoV-2 *in vitro*, to determine if it has potential as a reformulated, nasally administered or inhaled antiviral agent to help prevent spread of SARS-CoV-2 infection.

2. Materials and methods

2.1 Virus, cell culture, astodrimer sodium and controls

SARS-CoV-2 hCoV-19/Australia/VIC01/2020 was a gift from Melbourne's Peter Doherty Institute for Infection and Immunity (Melbourne, Australia). Virus stock was generated at 360Biolabs (Melbourne, Australia) by two passages in Vero cells in virus growth media, which comprised Minimal Essential Medium (MEM) without L-glutamine supplemented with 1% (w/v) L-glutamine, 1.0 µg/mL of L-(tosylamido-2-phenyl) ethyl chloromethyl ketone (TPCK)-treated trypsin (Worthington Biochemical, NJ, USA), 0.2% bovine serum albumin (BSA) and 1% insulin-transferrin-selenium (ITS).

Astodrimer sodium was prepared as 86.29 mg/mL in water and stored at 4°C. Astodrimer sodium has a molecular weight of 16581.57 g/mol and the structure is described and illustrated in Tyssen et al., 2010. The purity of the compound used in these studies was assessed by ultra-high-performance liquid chromatography (UPLC) to be 98.79%.

Remdesivir (MedChemExpress, NJ, USA) was used as a positive control in the virus-induced cytopathic effect (CPE) inhibition and time of addition (TOA) assays.

Hydroxychloroquine sulfate (Sigma-Aldrich, Sydney, Australia) was used as a positive control in the TOA assay.

2.2 Virus-induced cytopathic effect inhibition assay

African Green Monkey Kidney (Vero E6, ATCC-CRL1586) cell stocks were generated in cell growth medium, which comprised MEM without L-glutamine supplemented with 10% (v/v) heat-inactivated fetal bovine serum (FBS) and 1% (w/v) L-glutamine. Vero E6 cell monolayers were seeded in 96-well plates at $2x10^4$ cells/well in 100 µL growth medium (MEM supplemented with 1% (w/v) L-glutamine, 2% FBS) and incubated overnight at 37°C in 5% CO_2. SARS-CoV-2 infection was established by using a multiplicity of infection (MOI) of 0.05 to infect cell monolayers.

Astodrimer sodium or remdesivir were serially diluted 1:3, 9 times and each compound concentration was assessed for both antiviral efficacy and cytotoxicity in triplicate. Astodrimer sodium was added to Vero E6 cells 1 hour prior to infection or 1 hour post-infection with SARS-CoV-2. Cell cultures were incubated at 37°C in 5% CO_2 for 4 days prior to assessment of CPE. The virus growth media was MEM supplemented with 1% (w/v) L-glutamine, 2% FBS, and 4 µg/mL TPCK-treated trypsin. On Day 4, viral-induced CPE and cytotoxicity of the compound were determined by measuring the viable cells using the methylthiazolyldiphenyl-tetrazolium bromide (MTT) assay (MP Biomedicals, NSW, Australia). Absorbance was measured at 540-650 nm on a plate reader.

2.3 Virucidal assay

Astodrimer sodium was serially diluted 1:3, 9 times and tested in triplicate wells. SARS-CoV-2 was mixed with diluted astodrimer sodium at a MOI of 0.05 and incubated for 1 hour at 37°C in 5% CO_2. Virus and compound mixture were added to Vero E6 cell monolayers in 96-well plates and incubated at 37°C in 5% CO_2 for 4 days. On day 4, the virus-induced CPE was measured by the MTT assay as described above.

2.4 Determination of effective concentration (EC_{50} and EC_{90}) and cytotoxicity (CC_{50})

The concentration of compound that gives a 50% or 90% reduction in viral-induced CPE (EC_{50} or EC_{90} respectively) was calculated using the formula of Pauwels et al., 1998.

The concentration of compound that resulted in a 50% reduction in cell viability (CC_{50}) after 4 days of culture was also calculated by the formula of Pauwels et al., 1998.

2.5 Time of addition assay (TOA)

Vero E6 cell monolayers were grown in MEM supplemented with 1% (w/v) L-glutamine, 2% FBS. To ensure robust infection, cell cultures were infected with SARS-CoV-2 at a MOI of 1. The virus was adsorbed for 1 hour at 4°C, then parallel cultures were warmed to 37°C for 0 min, 15 min, 30 min, 60 min, 2 h, 4 h, 6 h prior to adding 0.345 mg/mL astodrimer sodium, 15 µM hydroxychloroquine, 5 µM remdesivir, or negative control (assay media only). For the 0 min time point, test or control articles were added immediately following virus pre-adsorption. Eight hours after virus infection (the duration of one cycle of replication), virus was harvested from the cells for each time point. The supernatant, containing virus, was retained and the virus titer determined for each time point via virus yield assay.

2.6 Virus yield reduction assay

Virus titer from the TOA study was quantified as a median tissue culture infective dose ($TCID_{50}$) value. $TCID_{50}$ is a measure of virus titer and represents the titer of a virus that produces infection in 50% of the tissue culture samples. Vero E6 cells monolayers were grown in MEM supplemented with 1% (w/v) L-glutamine, 2% FBS. Virus harvested from each time point was added to three wells and serially diluted three-fold across the plate for a total of nine different virus concentrations. Six of the wells contained assay media alone (i.e., no virus) and served as controls. Plates were incubated for three days and cell monolayers were then observed microscopically with visual scoring of virus-induced CPE used as an endpoint. The $TCID_{50}$ of the virus suspension was determined using the method of Reed-Muench, 1938. Virus yield was expressed as a percentage with respect to virus growth when no compound was added, for each time point.

3. Results

3.1 Virus-induced cytopathic effect inhibition assay

In two independent virus-induced CPE inhibition assays, astodrimer sodium inhibited SARS-CoV-2 (hCoV-19/Australia/VIC01/2020) replication in Vero E6 cells in a dose dependent manner (Table 1; Figure 1A, Figure 1B). Astodrimer sodium was active and inhibited viral replication when added either 1 hour prior to infection, or 1 hour post-infection with SARS-CoV-2.

Astodrimer sodium was initially tested in the range of 0.0013 to 8.63 mg/mL (0.078 to 520.4 µM). In the repeat set of assays, astodrimer sodium was tested in the range of 0.0001 to 0.86 mg/mL (0.008 to 52.0 µM) to help further characterize the lower end of the dose response

curve. The effective and cytotoxic concentrations, and selectivity indices from the assays are shown individually and as means in Table 1.

The selectivity index (SI) for astodrimer sodium against SARS-CoV-2 ranged from 793 to 2197 for the initial assays where compound was added 1 hour prior to infection and 1 hour after infection, respectively, and was >70 to >80 in the repeat assays, in which cytotoxicity was not observed up to the highest concentration tested (0.86 mg/mL).

The positive control, remdesivir, was also active in the CPE inhibition assay, with a SI of >33.

3.2 Virucidal assay

A second study was performed to determine if astodrimer sodium was able to reduce viral infectivity by binding to SARS-CoV-2 directly prior to infection of Vero E6 cells. Astodrimer sodium treatment demonstrated a similar level of antiviral efficacy to the CPE studies (Table 1; Figure 1C) with an EC_{50} of 1.83 µM (0.030 mg/mL) and SI of 130; n=1.

3.3 Time of addition assay (TOA)

To further investigate the mechanism of action of astodrimer sodium, a TOA study was performed. Compound was added to virus-infected cells at early, middle and late stages of the SARS-CoV-2 replication lifecycle, which is completed in approximately 8 hours (Ogando et al., 2020). The addition of 0.345 mg/mL astodrimer sodium at times ranging from 0 min to 6 h post-infection resulted in virus levels below the lower limit of detection at every time point (Figure 2). This finding was in contrast to detectable infectious virus levels at all equivalent time points in the positive control (remdesivir and hydroxychloroquine sulfate) and virus only cultures. Hydroxychloroquine sulfate had no discernible effect on virus replication at any time point at 15

μM. Remdesivir (5 μM, ~5-10 times the EC_{50}) inhibited virus replication by <1 log_{10} $TCID_{50}$ when added within 15 or 30 min post-infection.

4. Discussion

Astodrimer sodium demonstrated potent antiviral activity against SARS-CoV-2 in Vero E6 cells. The finding of antiviral activity was demonstrated when astodrimer sodium was added to cells or mixed with SARS-CoV-2 prior to infection of cells, when the compound was added to cells already exposed to SARS-CoV-2, and when astodrimer sodium was added at all times throughout the SARS-CoV-2 replication lifecycle to cells already infected with virus.

Of note is a significantly high SI for astodrimer sodium relative to other antiviral compounds under investigation for SARS-CoV-2 activity (Pizzorno et al., 2020).

Remdesivir was used as the antiviral positive control for the CPE inhibition assays and the experimental EC_{50} was consistent with published data generated with a different clinical isolate of SARS-CoV-2 (Wang et al., 2020).

The antiviral data are consistent with astodrimer sodium being a potent inhibitor of early events in the virus lifecycle. The virucidal assay data suggest that astodrimer sodium antiviral activity was consistent with the proposed mechanism of action of binding to virus, thereby inactivating virus and blocking infection.

The complete abolition of virus infection at all time points in the TOA assay are also consistent with astodrimer sodium being a potent antiviral agent that inhibits the early phase of virus infection and replication. These findings suggest potent inhibition of viral attachment, fusion and entry of the virus, which prevents virus replication and release of infectious virus progeny. It is

possible that potential carryover of compound from the initial cell culture supernatant to the cultures used in the virus-yield reduction assay may have affected the TOA data. Additional studies may further demonstrate the mechanism of action of astodrimer sodium inhibition of SARS-CoV-2 replication.

However, astodrimer sodium has been previously found to be an effective antiviral that exerts its inhibition in the early virus-host receptor recognition interactions (Tyssen et al., 2010; Telwatte et al., 2011), and its potential mechanism of action against SARS-CoV-2 is likely to be similar to that identified for other pathogens. Astodrimer sodium was found to bind to HIV-1 by strong electrostatic forces to positively charged clusters of highly conserved amino acids on HIV-1 gp120 protein and/or positively charged amino acid regions located between the stems of V1/V2 and V3 loops, which are exposed by conformational changes to gp120 after viral binding to the receptor/co-receptor complex (Tyssen et al., 2010; Connell and Lortat-Jacob, 2013).

Many viruses utilize negatively charged heparan sulfate proteoglycans (HS) on the cell plasma membrane as an initial means to scan the surface of the cell, and to attach in order to chaperone the virus onto the receptor complex prior to viral entry (Sarrazin et al., 2011; Connell and Lortat-Jacob, 2013). The receptor interactions occur in a sequential manner with virus-HS interactions preceding receptor/co-receptor binding, which combined leads to fusion of the viral envelope and the cell membrane.

Data indicate that astodrimer sodium-gp120 interaction may physically block initial HIV-1 association with HS and thereby block the subsequent virus-receptor complex functions. Virucidal studies of astodrimer sodium determined that it did not disrupt the HIV-1 particle or cause the loss of gp120 spike protein from the viral surface (Telwatte et al., 2011).

A recent report by Liu et al., 2020, has described that densely glycosylated trimeric SARS-CoV-2 spike (S) protein subunit S1, which is important for receptor binding, binds to HS. To engage with the angiotensin converting enzyme 2 (ACE2) receptor, the S protein undergoes a hinge-like conformational change that transiently hides or exposes the determinants of receptor binding (Wrapp et al., 2020). Recent studies have identified the binding of heparin to the receptor binding domain (RBD) of S1 resulting in a conformational change to the S protein (Mycroft-West et al., 2020a, b and c). Mutations in the S protein that are distal from the RBD also impact on viral transmission (Walls et al., 2020; Korber et al., 2020; Yuan et al., 2020). Non-RBD polybasic cleavage sites, including S1/S2 loop (Hoffman et al., 2020a), have been described on SARS-CoV-2 S protein (Qiao and Olvera de la Cruz, 2020) and may also be a site of potential interaction with astodrimer sodium.

SARS-CoV-2 utilizes the ACE2 receptor for viral infection of host cells (Hoffmann et al., 2020b). Human CoV-NL63 also utilizes HS and ACE2 as its cellular receptor complex (Milewska et al., 2014). The importance of HS for viral infectivity was also demonstrated for close genetically related pseudo-typed SARS-CoV (Lang et al., 2011). The potential dependence of SARS-CoV-2 on HS for attachment and entry combined with antiviral data from other viruses suggest that negatively charged astodrimer sodium may have antiviral activity against SARS-CoV-2 *in vitro* by blocking the early virus-receptor recognition events.

Astodrimer sodium is a polyanionic dendrimer currently being reformulated for potential use as a topical, nasally administered antiviral agent to help prevent acquisition and transmission of SARS-CoV-2 infection. The potential advantages of astodrimer sodium over other technologies include its lack of systemic absorption following topical application (Chen et al., 2009; O'Loughlin et al., 2010; McGowan et al., 2011). In addition, the SI of astodrimer sodium for

SARS-CoV-2 is high and in a vaginal gel formulation (10 mg/mL), the compound has been shown to be safe and effective in phase 2 and large phase 3 trials for treatment and prevention of BV (Schwebke et al., 2019; Chavoustie et al., 2020; Waldbaum et al., 2020) and is now marketed in Europe, Australia, New Zealand and several countries in Asia. Astodrimer sodium is also the active antiviral substance in VivaGel® condom products that have marketing authorization in Europe, Japan, Australia/New Zealand and Canada. However, these current formulations are not appropriate for use to protect the respiratory tract from SARS-CoV-2 infection.

5. Conclusions

These data from the current studies, taken together with studies of astodrimer sodium antiviral activity against HIV-1 and HSV-1 and -2, indicate that the compound exerts its antiviral activity against SARS-CoV-2 by interfering with the early virus-cell recognition events. When applied 1 hour post-infection through 6 hours post-infection, astodrimer sodium may prevent early virus entry steps such as attachment, thereby reducing or preventing viral infection or cell-cell spread.

In the absence of universally effective antiviral agents and/or vaccines against SARS-CoV-2, there is a need to develop a preventive therapy that could be used to significantly reduce the transmission of the virus. An antiviral agent such as astodrimer sodium that blocks binding of the virus to target cells could potentially be used as a preventive and/or a therapeutic agent. These antiviral studies suggest that a reformulation of astodrimer sodium for delivery to the respiratory tract may be an effective preventive strategy to block SARS-CoV-2 transmission and augment other protective and therapeutic strategies.

The potent antiviral activity of astodrimer sodium against SARS-CoV-2 warrants further investigation.

Table

Table 1: Antiviral efficacy, measured by a reduction in CPE in virus-infected cells, and selectivity of astodrimer sodium against SARS-CoV-2 (hCoV-19/Australia/VIC01/2020) infection of Vero E6 cells

Compound / Assay Type	Repeat	EC_{50}		EC_{90}		CC_{50}		SI
		µM	mg/mL	µM	mg/mL	µM	mg/mL	
Astodrimer sodium added 1-hour pre-infection	Assay 1	0.223	0.004	0.233	0.004	177	2.93	793
	Assay 2	0.742	0.012	7.03	0.117	>52.0	>0.863	>70
	Mean ± SD	0.482 ± 0.367	0.008 ± 0.006	3.63 ± 4.80	0.060 ± 0.080	NC	NC	>431[a]
Astodrimer sodium added 1-hour post-infection	Assay 1	0.090	0.002	0.175	0.003	199	3.29	2197
	Assay 2	0.651	0.011	10.1	0.168	>52.0	>0.863	>80
	Mean ± SD	0.371 ± 0.397	0.006 ± 0.007	5.15 ± 7.03	0.085 ± 0.117	NC	NC	>1138[a]
Virucidal: SARS-CoV-2 mixed with astodrimer sodium 1-hour pre-infection	Assay 1	1.83	0.030	3.70	0.061	237	3.93	130
Remdesivir	Assay 1	0.59	N/A	1.20	N/A	>20	N/A	>33
	Assay 2	0.61	N/A	1.51	N/A	>20	N/A	>33

EC_{50}=50% effective concentration; EC_{90}=90% effective concentration; CC_{50}=50% cytotoxic concentration; SI=selectivity index (CC_{50}/EC_{50}); SD=standard deviation; NC=not calculated; N/A=not applicable

[a] Average of Assay 1 and Assay 2 SI

Figure Captions

Figure 1. Dose-response analysis of the antiviral activity of astodrimer sodium

Dose-response curves of the antiviral activity as measured by a reduction in CPE on Day 4 by astodrimer sodium against SARS-CoV-2 (hCoV-19/Australia/VIC01/2020) replication in Vero E6 cells, and cell viability as percent of cell control. **A.** Cell cultures infected one-hour pre-infection – Assay 1 (left panel) and Assay 2 (right panel). **B.** Cell cultures infected one-hour post-infection – Assay 1 (left panel) and Assay 2 (right panel). **C.** Virus and astodrimer sodium mixed for one hour prior to infection of cell cultures. EC_{50} and CC_{50} values and selectivity indices are indicated. Points and error bars represent mean ± SD of triplicate readings.

Figure 2. Time of addition experiment

Astodrimer sodium (0.345 mg/mL; blue), Remdesivir (5 µM; red), Hydroxychloroquine sulfate (15 µM; green) and SARS-CoV-2 (hCoV-19/Australia/VIC01/2020) only (black) were assessed for antiviral activity at early middle and late stages of virus replication by adding compounds at different times post-infection (0 min, 15 min, 30 min, 1 h, 2 h, 4 h, and 6 h). The amount of virus secreted into the supernatant at 8 hours post-infection was determined by $TCID_{50}$. Each point on the graph represents the virus titer present after one cycle of replication following addition of compound at the indicated time following virus infection. Infectious virus titer for astodrimer sodium was below the lower limit of detection (LLOD) at all time points.

Fig. 1

A

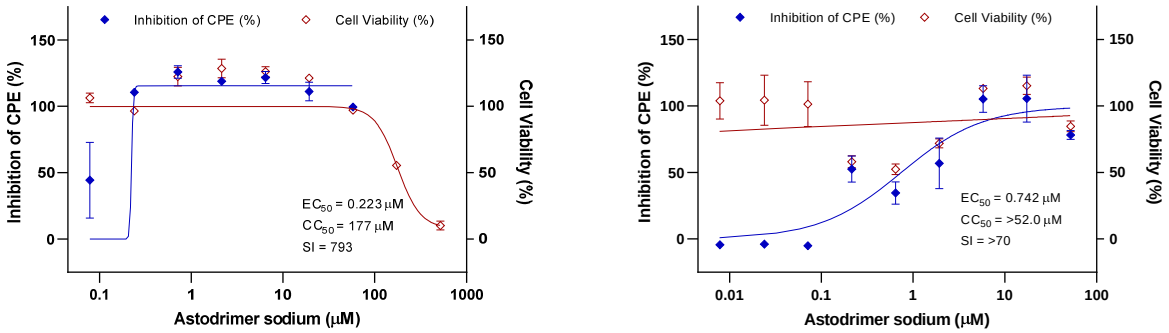
Inhibition of CPE (%)
Cell Viability (%)
Inhibition of CPE (%)
Cell Viability (%)
Astodrimer sodium (μM)
EC50 = 0.223 μM
CC50 = 177 μM
SI = 793
Inhibition of CPE (%)
Cell Viability (%)
Inhibition of CPE (%)
Cell Viability (%)
Astodrimer sodium (μM)
EC50 = 0.742 μM
CC50 = >52.0 μM
SI = >70

B

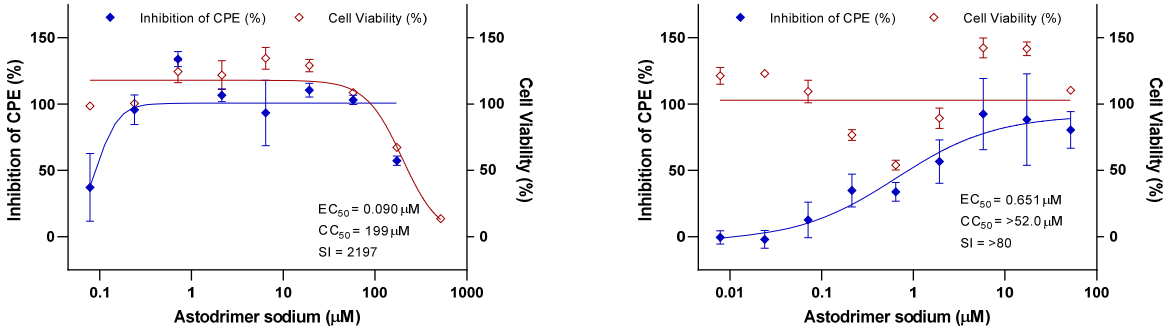
Inhibition of CPE (%)
Cell Viability (%)
Inhibition of CPE (%)
Cell Viability (%)
Astodrimer sodium (μM)
EC50 = 0.090 μM
CC50 = 199 μM
SI = 2197
Inhibition of CPE (%)
Cell Viability (%)
Inhibition of CPE (%)
Cell Viability (%)
Astodrimer sodium (μM)
EC50 = 0.651 μM
CC50 = >52.0 μM
SI = >80

C

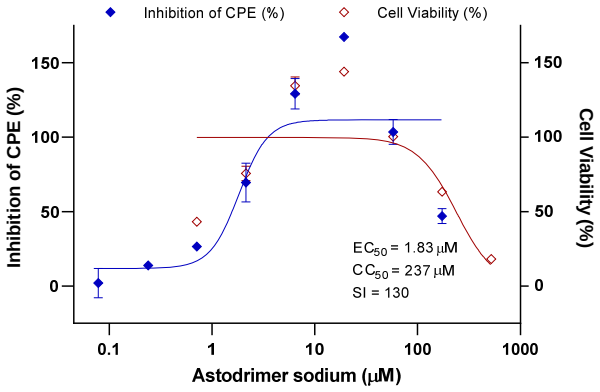
Inhibition of CPE (%)
Cell Viability (%)
Inhibition of CPE (%)
Cell Viability (%)
Astodrimer sodium (μM)
EC50 = 1.83 μM
CC50 = 237 μM
SI = 130

Fig. 2

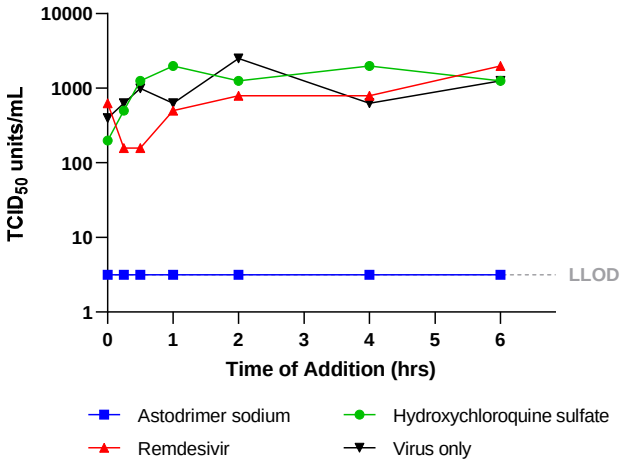
10000
1000
100
10
1
TCID50 units/mL
LLOD
0
1
2
3
4
5
6
Time of Addition (hrs)
Astodrimer sodium
Hydroxychloroquine sulfate
Remdesivir
Virus only

Abbreviations

ACE2	angiotensin converting enzyme 2	MOI	multiplicity of infection
BSA	bovine serum albumin	MTT	methylthiazolyldiphenyl-tetrazolium bromide
BV	bacterial vaginosis	NC	not calculated
CC_{50}	50% cytotoxic concentration	RBD	receptor binding domain
COVID-19	coronavirus disease 2019	S protein	spike protein
CPE	cytopathic effect	SARS-CoV	severe acute respiratory syndrome coronavirus
EC_{50}	50% effective concentration	SARS-CoV-2	severe acute respiratory syndrome coronavirus 2
FBS	fetal bovine serum	SD	standard deviation
HIV-1	human immunodeficiency virus type 1	SHIV	simian-human immunodeficiency virus
HPV	human papillomavirus	SI	selectivity index
HS	heparan sulfate proteoglycan	$TCID_{50}$	median tissue culture infective dose
HSV	herpes simplex virus	TOA	time of addition
ITS	insulin-transferrin-selenium	TPCK	L-(tosylamido-2-phenyl) ethyl chloromethyl ketone
LLOD	lower limit of detection	UPLC	ultra-high-performance liquid chromatography
MEM	minimal essential medium		

Acknowledgments

The authors were fully responsible for the content, editorial decisions, and opinions expressed in the current article. The authors would like to acknowledge 360Biolabs Pty Ltd (Melbourne, Australia) for the conduct of the assays, collection of data, and provision of materials other than astodrimer sodium. The authors would also like to thank the Peter Doherty Institute for Infection and Immunity (Melbourne, Australia) for the gift to 360Biolabs of SARS-CoV-2 hCoV-19/Australia/VIC01/2020 used in these studies.

Funding

The research was funded by Starpharma Pty Ltd, which was responsible for study design, interpretation of data, writing the manuscript and decision to submit the article for publication.

References

Bernstein, D.I., Stanberry, L.R., Sacks, S., Ayisi, N.K., Gong, Y.H., Ireland, J., Mumper, R.J., Holan, G., Matthews, B, McCarthy, T., Bourne, N., 2003. Evaluations of unformulated and formulated dendrimer-based microbicide candidates in mouse and guinea pig models of genital herpes. Antimicrob. Agents Chemother. 47(12), 3784-3788. https://doi.org/10.1128/aac.47.12.3784-3788.2003

Chavoustie, S.E., Carter, B.A., Waldbaum, A.S., Donders, G.G.G., Peters, K.H., Schwebke, J.R., Paull, J.R.A, Price, C.F., Castellarnau, A., McCloud, P., Kinghorn, G.R., 2020. Two phase 3, double-blinded, placebo-controlled studies of the efficacy and safety of Astodrimer 1% Gel for the treatment of bacterial vaginosis. Eur. J. Obstet. Gynecol. Reprod. Biol. 245, 13-18. https://doi.org/10.1016/j.ejogrb.2019.11.032

Chen, M.Y., Millwood, I.Y., Wand, H., Poynten, M, Law, M., Kaldor, J.M., Wesselingh, S., Price, C.F., Clark, L.J., Paull, J.R., Fairley, C.K., 2009. A randomized controlled trial of the safety of candidate microbicide SPL7013 gel when applied to the penis. J. Acquir. Immune Defic. Syndr. 50(4), 375-380. https://doi.org/10.1097/QAI.0b013e318198a7e6

Connell, B.J., Lortat-Jacob, H., 2013. Human immunodeficiency virus and heparan sulfate: from attachment to entry inhibition. Frontiers Immunol. 4, 385. https://doi.org/10.3389/fimmu.2013.00385

Gong, E., Matthews, B., McCarthy, T., Chu, J., Holan, G., Raff, J., Sacks, S., 2005. Evaluation of dendrimer SPL7013, a lead microbicide candidate against herpes simplex virus. Antiviral Res. 68(3), 139-146. https://doi.org/10.1016/j.antiviral.2005.08.004

Hoffmann M., Kleine-Weber, H., Pöhlmann, S., 2020a. A multibasic cleavage site in the spike protein of SARS-CoV-2 is essential for infection of human lung cells. Molecular Cell 78(4), 779-784.e5. https://doi.org/10.1016/j.molcel.2020.04.022

Hoffmann, M., Kleine-Weber, H., Schroeder, S., Krüger, N., Herrler, T., Erichsen, S., Schiergens, T.S., Herrler, G., Wu, N.H., Nitsche, A., Müller, M.A., Drosten, C., Pöhlmann, S., 2020b. SARS-CoV-2 cell entry depends on ACE2 and TMPRSS2 and is blocked by a clinically proven protease inhibitor. Cell 181(2), 271-280.e8. https://doi.org/10.1016/j.cell.2020.02.052

Hou, Y.J., Okuda, K., Edwards, C.E., et al. 2020. SARS-CoV-2 reverse genetics reveals a variable infection gradient in the respiratory tract. Cell 182(2), 429-446.e14. https://doi.org/10.1016/j.cell.2020.05.042

Jiang, Y.H., Emau, P., Cairns, S., Flanary, L., Morton, W.R., McCarthy, T., Tsai, C.C., 2005.

SPL7013 gel as a topical microbicide for prevention of vaginal transmission of $SHIV_{89.6P}$ in macaques. AIDS Res. Hum. Retroviruses 21(3), 207-213. https://doi.org/10.1089/aid.2005.21.207

Korber, B., Fischer, W.M., Gnanakaran, S., Yoon, H., Theiler, J., Abfalterer, W., Foley, B., Giorgi, E.E., Bhattacharya, T., Parker, M.D., Partridge, D.G., Evans, C.M., de Silva, T.I., LaBranche, C.C., Montefiori, D.C., 2020. Spike mutation pipeline reveals the emergence of a more transmissible form of SARS-CoV-2. bioRxiv. https://doi.org/10.1101/2020.04.29.069054

Lackman-Smith, C., Osterling, C., Luckenbaugh, K., Mankowski, M., Snyder, B., Lewis, G., Paull, J., Profy, A., Ptak, R.G., Buckheit Jr., R.W., Watson, K.M., Cummins Jr., J.E., Sanders-Beer, B.E., 2008. Development of a comprehensive human immunodeficiency virus type-1 screening algorithm for discovery and preclinical testing of topical microbicides. Antimicrob. Agents Chemother. 52(5), 1768-1781. https://doi.org/10.1128/AAC.01328-07

Lang, J., Yang, N., Deng, J., Liu, K., Yang, P., Zhang, G., Jiang, C., 2011. Inhibition of SARS pseudovirus cell entry by lactoferrin binding to heparan sulfate proteoglycans. PLoS ONE 6(8), e23710. https://doi.org/10.1371/journal.pone.0023710

Liu, L., Chopra, P., Li, X., Wolfert, M.A., Tompkins, S.M., Boons, G.J., 2020. SARS-CoV-2 spike protein binds heparan sulfate in a length- and sequence-dependent manner. bioRxiv. https://doi.org/10.1101/2020.05.10.087288

McCarthy, T.D., Karellas, P., Henderson, S.A., Giannis, M., O'Keefe, D.F., Heery, G., Paull, J.R.A., Matthews, B.R., Holan, G., 2005. Dendrimers as drugs: discovery and preclinical

and clinical development of dendrimer microbicides for HIV and STI prevention. Mol. Pharm. 2(4), 312-318. https://doi.org/10.1021/mp050023q

McGowan, I., Gomez, K., Bruder, K., Febo, I., Chen, B.A., Richardson, B.A., Husnik, M., Livant, E., Price, C., Jacobson, C., 2011. Phase 1 randomized trial of the vaginal safety and acceptability of SPL7013 gel (VivaGel®) in sexually active young women (MTN-004). AIDS 25(8), 1057-1064. https://doi.org/10.1097/QAD.0b013e328346bd3e

Milewska, A., Zarebski, M., Nowak, P., Stozek, K., Potempa, J., Pyrc, K., 2014. Human coronavirus NL63 utilizes heparan sulfate proteoglycans for attachment to target cells. J. Virol. 88(22), 13221-13230. https://doi.org/10.1128/JVI.02078-14

Mycroft-West, C., Su, D., Elli, S., Li, Y., Guimond, S., Miller, G., Turnbull, J., Yates, E., Guerrini, M., Fernig, D., Lima, M., Skidmore, M., 2020a. The 2019 coronavirus (SARS-CoV-2) surface protein (spike) S1 receptor binding domain undergoes conformational change upon heparin binding. bioRxiv. https://doi.org/10.1101/2020.02.29.971093

Mycroft-West, C.J., Su, D., Li, Y., Guimond, S., Rudd, T.R., Elli, S., Miller, G., Nunes, Q.M., Procter, P., Bisio, A., Forsyth, N.R., Turnbull, J.E., Guerrini, M., Fernig, D., Yates, E.A., Lima, M.A., Skidmore, M.A., 2020b. SARS CoV-2 spike S1 receptor binding domain undergoes conformational change upon interaction with low molecular weight heparins. bioRxiv. https://doi.org/10.1101/2020.04.29.068486

Mycroft-West, C.J., Su, D., Pagani, I., Rudd, T.R., Elli, S., Guimond, S., Miller, G., Meneghetti, M.C.Z., Nader, H.B., Li, Y., Nunes, Q.M., Procter, P., Mancini, N., Clementi, M., Forsyth, N.R., Turnbull, J.E., Guerrini, M., Fernig, D., Vicenzi, E., Yates, E.A., Lima, M.A., Skidmore, M.A., 2020c. Heparin inhibits cellular invasion of SARS-CoV-2: structural

dependence on the interaction of the surface protein (spike) S1 receptor binding domain with heparin. bioRxiv 2020.2004.2028.066761. https://doi.org/10.1101/2020.04.28.066761

O'Loughlin, J., Millwood, I.Y., McDonald, H.M., Price, C.F., Kaldor, J.M., Paull, J.R.A., 2010. Safety, tolerability, and pharmacokinetics of SPL7013 gel (VivaGel®): a dose ranging phase 1 study. Sex. Transm. Dis. 37(2), 100-104. https://doi.org/10.1097/OLQ.0b013e3181bc0aac

Ogando, N.S., Dalebout, T.J., Zevenhoven-Dobbe, J.C., Limpens, R.W.A.L., van der Meer, Y., Caly, L., Druce, J., de Vries, J.J.C., Kikkert, M., Bárcena, M., Sidorov, I., Snijder, J., 2020. SARS-coronavirus-2 replication in Vero E6 cells: replication kinetics, rapid adaption and cytopathology. J. General Virol. 10.1099/jgv.0.001453. Advance online publication. https://doi.org/10.1099/jgv.0.001453

Pauwels, R., Balzarini, J., Baba, M., Snoeck, R., Schols, D., Herdewijn, P., Desmyter, J., De Clercq, E., 1988. Rapid and automated tetrazolium-based colorimetric assay for the detection of anti-HIV compounds. J. Virol. Methods 20(4), 309-321. https://doi.org/10.1016/0166-0934(88)90134-6

Pizzorno, A., Padey, B., Dubois, J., Julien, T., Traversier, A., Dulière, V., Brun, P., Lina, B., Rosa-Calatrava, M., Terrier, O., 2020. In vitro evaluation of antiviral activity of single and combined repurposable drugs against SARS-CoV-2. Antiviral Res. 104878. Advance online publication. https://doi.org/10.1016/j.antiviral.2020.104878

Qiao, B., Olvera de la Cruz, M., 2020. The distal polybasic cleavage sites of SARS-CoV-2 spike protein enhance spike protein-ACE2 binding. bioRxiv June 10. https://doi.org/10.1101/2020.06.09.142877

Reed, L.J., Muench, H., 1938. A simple method of estimating fifty percent endpoints. Am. J. Hyg. 27(3), 493-497. https://doi.org/10.1093/oxfordjournals.aje.a118408

Sarrazin, S., Lamanna, W.C., Esko, J.D., 2011. Heparan sulfate proteoglycans. Cold Spring Harb. Perspect. Biol. 3(7), a004952. https://doi.org/10.1101/cshperspect.a004952

Schwebke, J., Carter, B., Waldbaum, A., Price, C., Castellarnau, A., Paull, J., McCloud, P., Kinghorn, G., 2019. Results of a phase 3, randomized, double-blind, placebo controlled study to evaluate the efficacy and safety of astodrimer gel for prevention of recurrent bacterial vaginosis. Am. J. Obstet. Gynecol. 221(6), 672-673. https://doi.org/10.1016/j.ajog.2019.10.087

Sungnak, W., Huang, N., Bécavin, C., Berg, M., Queen, R., Litvinukova, M., Talavera-López, C., Maatz, H., Reichart, D., Sampaziotis, F., Worlock, K.B., Yoshida, M., Barnes, J.L., 2020. SARS-CoV-2 entry factors are highly expressed in nasal epithelial cells together with innate immune genes. Nat. Med. 26(5), 681-687. https://doi.org/10.1038/s41591-020-0868-6

Telwatte, S., Moore, K., Johnson, A., Tyssen, D., Sterjovski, J., Aldunate, M., Gorry, P.R., Ramsland, P.A., Lewis, G.R., Paull, J.R.A., Sonza, S., Tachedjian, G., 2011. Virucidal activity of the dendrimer microbicide SPL7013 against HIV-1. Antiviral Res. 90(3), 195-199. https://doi.org/10.1016/j.antiviral.2011.03.186

Tyssen, D., Henderson, S.A., Johnson, A., Sterjovski, J, Moore, K., La, J., Zanin, M., Sonza, S., Karellas, P., Giannis, M.P., Krippner, G., Wesselingh, S., McCarthy, T., Gorry, P.R., Ramsland, P.A., Cone, R., Paull, J.R.A., Lewis, G.R., Tachedjian, G., 2010. Structure

activity relationship of dendrimer microbicides with dual action antiviral activity. PLoS ONE 5(8), e12309. https://doi.org/10.1371/journal.pone.0012309

Waldbaum, A.S., Schwebke, J.R., Paull, J.R.A., Price, C.F., Edmondson, S.R., Castellarnau, A., McCloud, P., Kinghorn, G.R., 2020. A phase 2, double-blind, multicenter, randomized, placebo-controlled, dose-ranging study of the efficacy and safety of Astodrimer Gel for the treatment of bacterial vaginosis. PLoS ONE 15(5), e0232394. https://doi.org/10.1371/journal.pone.0232394

Walls, A.C., Park, Y.J., Tortorici, M.A., Wall, A., McGuire, A.T., Veesler, D., 2020. Structure, function and antigenicity of the SARS-CoV-2 spike glycoprotein. Cell 181(2), 281-292.e6 https://doi.org/10.1016/j.cell.2020.02.058

Wang, M., Cao, R., Zhang, L., Yang, X., Liu, J., Xu, M/., Shi, Z., Hu, Z., Zhong, W., Xiao, G., 2020. Remdesivir and chloroquine effectively inhibit the recently emerged novel coronavirus (2019-nCoV) in vitro. Cell Res. 30(3), 269-271. https://doi.org/10.1038/s41422-020-0282-0

Wrapp, D., Wang, N., Corbett, K.S., Goldsmith, J.A., Hsieh, C.L., Abiona, O., Graham, B.S., McLellan, J.S., 2020. Cryo-EM structure of the 2019-nCoV spike in the prefusion conformation. Science 367(6483), 1260-1263. https://doi.org/10.1126/science.abb2507

Yuan, M., Wu, N.C., Zhu, X., Lee, C.C.D., So, R.T.Y., Lv, H., Mok, C.K.P., Wilson, I.A., 2020. A highly conserved cryptic epitope in the receptor binding domains of SARS-CoV-2 and SARS-CoV. Science 368(6491), 630-633. https://doi.org/10.1126/science.abb7269